Original Article

Intrinsic pulmonary sealing, its mechanisms and impact on validity and translational value of lung sealant studies: a pooled analysis of animal studies

Bob P. Hermans[1]^, Wilson W. L. Li[1], Edwin A. Roozen[2], Daniël I. M. van Dort[1], Shoko Vos[3], Stefan M. van der Heide[1], Erik H. F. M. van der Heijden[4], Richard P. G. ten Broek[2], Harry van Goor[2], Ad F. T. M. Verhagen[1]

[1]Department of Cardio-Thoracic Surgery, Radboud University Medical Center, Radboud Institute for Health Sciences, Nijmegen, The Netherlands; [2]Department of General Surgery, Radboud University Medical Center, Radboud Institute for Health Sciences, Nijmegen, The Netherlands; [3]Department of Pathology, Radboud University Medical Center, Radboud Institute for Health Sciences, Nijmegen, The Netherlands; [4]Department of Pulmonology, Radboud University Medical Center, Radboud Institute for Health Sciences, Nijmegen, The Netherlands

Contributions: (I) Conception and design: BP Hermans, WWL Li, EA Roozen, DIM van Dort, SM van der Heide, H van Goor, AFTM Verhagen; (II) Administrative support: BP Hermans, DIM van Dort; (III) Provision of study materials or patients: BP Hermans, EA Roozen, DIM van Dort; (IV) Collection and assembly of data: BP Hermans, EA Roozen, DIM van Dort; (V) Data analysis and interpretation: BP Hermans, S Vos, DIM van Dort, WWL Li, RPG ten Broek, H van Goor, AFTM Verhagen; (VI) Manuscript writing: All authors; (VII) Final approval of manuscript: All authors.

Correspondence to: Bob P. Hermans, BSc. Department of Cardio-Thoracic Surgery, Radboud University Medical Center, Radboud Institute for Health Sciences, Geert Grooteplein Zuid 10, 6525 GA, Nijmegen, The Netherlands. Email: Bob.Hermans@Radboudumc.nl.

Background: No validated and standardized animal models of pulmonary air leakage (PAL) exist for testing aerostatic efficacy of lung sealants. Lack of negative control groups in published studies and intrinsic sealing mechanisms of healthy animal lungs might contribute to a translational gap, leading to poor clinical results. This study aims to address the impact of intrinsic sealing mechanisms on the validity of PAL models, and investigate the conditions required for an ovine model of PAL for lung sealant testing.

Methods: An ovine acute aerostasis model was developed, consisting of a bilateral thoracotomy with lesion creation, chest tube insertion and monitoring of air leaks using digital drains (≥80 minutes), under spontaneous respiration. Healthy mixed-breed adult female sheep were used and all *in vivo* procedures were performed under terminal anesthesia. Superficial parenchymal lesions were tested *post-mortem* and *in vivo*, extended lesions including bronchioles (deep bowl-shaped and sequential lung amputation lesions) were tested *in vivo*. Experiment outcomes include air leakage (AL), minimal leaking pressure (MLP) and histology.

Results: Two *post-mortem* (N=4 superficial parenchymal lesions) and 10 *in vivo* experiments (N=5 superficial parenchymal and N=16 lesions involving bronchioles) were performed. In contrast to the *post-mortem* model, superficial parenchymal lesions *in vivo* showed less air leak [mean flow ± standard deviation (SD): 760±693 *vs.* 42±33 mL/min, P=0.055]. All superficial parenchymal lesions *in vivo* sealed intrinsically within a median time of 20 minutes [interquartile range (IQR), 10–75 minutes]. Histology of the intrinsic sealing layer revealed an extended area of alveolar collapse below the incision with intra-alveolar hemorrhage. Compared to superficial parenchymal lesions *in vivo*, lesions involving bronchioles induced significantly higher air leak post-operatively (normalized mean flow ± SD: 459±221 mL/min, P=0.003). At termination, 5/9 (55.6%) were still leaking (median drain time: 273 minutes, IQR, 207–435 minutes), and intrinsic sealing for the remaining lungs occurred within a median of 115 minutes (IQR, 52–245 minutes).

Conclusions: Lung parenchyma of healthy sheep shows a strong intrinsic sealing mechanism, explained pathologically by an extended area of alveolar collapse, which may contribute to a translational gap in lung sealant research. A meaningful ovine model has to consist of deep lesions involving bronchioles of >ø1.5 mm.

^ ORCID: 0000-0001-8586-063X.

Further research is needed to develop a standardized PAL model, to improve clinical effectiveness of lung sealants.

Keywords: Air leak; lung sealant; lung surgery; animal model; experimental

Submitted Feb 22, 2023. Accepted for publication Jul 28, 2023. Published online Aug 30, 2023.
doi: 10.21037/jtd-23-180
View this article at: https://dx.doi.org/10.21037/jtd-23-180

Introduction

Prolonged pulmonary air leak (pPAL) occurs in up to 30% of lung resections, causing increased morbidity (empyema and post-operative complications), reinterventions (4.8%), readmissions [odds ratio (OR) =2] and mortality (OR =1.9) (1-7). Preclinical animal studies with lung sealants have shown promising results, and 74% of surgeons use sealants in their high-risk patients (8-10). Results of lung sealants in preventing pPAL in clinical studies, however, are mixed and guidelines do not recommend their routine use (11-16). Recently, in a European Society of Thoracic Surgeons (ESTS) survey, the majority of the 258 responding thoracic surgeons affirmed the lack of sufficient evidence for lung sealants, and an unmet clinical need for more effective lung sealants was described (17). The marked discrepancy between the more positive preclinical studies and often unsatisfactory clinical results indicate a potential translational gap.

For effective clinical use, the performance of lung sealants should be investigated during their development in properly validated animal models. For a valid model, pulmonary air leakage (PAL) needs to be present of sufficient magnitude and without the capacity to resolve spontaneously for the study duration, ensuring accurate assessment of both acute and prolonged aerostatic efficacy of applied lung sealants. Furthermore, in contrast to patients undergoing lung resections, animals used in lung sealing experiments are healthy in 92% of cases and may poses enhanced intrinsic sealing and regenerative capacities, which can possibly invalidate positive study findings if unaccounted for (18-20). In the present literature, no standardized animal model exists that guarantees clinically significant pPAL, and negative control groups were only used in 18.7% of preclinical studies (20,21). Therefore, the validity of many previously tested lesions for pPAL in animal models is unknown (20,22,23).

Several enhancements to animal models for lung surgery research have been described, that might reduce the translational gap. First of all, the type of lesion might impact PAL, as larger lesions and lesions involving bronchioles seem more likely to result in pPAL (21,24). Secondly, disease models have been described, including models for emphysema and heparinized models (25,26). Although these disease models increase the risk of pPAL, these models may come at the cost of increased variation and decreased animal welfare. In the present study, we assessed the impact of different types of lesions on PAL from the results of negative controls (untreated lesions) in three animal experiments. These results provide insight in the impact of intrinsic sealing mechanisms on the validity and translational value of animal models for lung sealant research. We present this article in accordance with the ARRIVE reporting checklist (available at https://jtd.amegroups.com/article/view/10.21037/jtd-23-180/rc).

Highlight box

Key findings

- Superficial lesions in healthy sheep lungs show a rapid intrinsic sealing mechanism, which invalidates these lesions for use in lung sealing studies. Sequential amputation lesions including bronchioles of >ø1.5 mm may be a suitable alternative for acute testing of aerostatic sealant effectiveness.

What is known and what is new?

- There is no standardized *in vivo* model of pulmonary air leakage, and current models are heterogenous. There is some evidence for intrinsic sealing mechanisms in healthy animal lungs, which may cause a translational gap in lung sealant research.
- This study demonstrates the existence of intrinsic sealing in healthy animal lungs, offers novel insights into its mechanisms and confirms the possibility of a translational gap in preclinical studies.

What is the implication, and what should change now?

- Researchers should control for intrinsic sealing mechanisms using negative controls when investigating lung sealants in preclinical studies, to demonstrate treatment effectiveness. To this end, a standardized model of pulmonary air leakage is a prerequisite.

Methods

Study setup

The intrinsic sealing capacities of both superficial parenchymal lesions and lesions involving bronchioles are investigated in *in vivo* and *post-mortem* ovine models, by measuring air leakage (AL) and characterizing the responsible mechanisms histopathologically. To simulate a real post-operative scenario, an ovine acute aerostasis model with both mechanical ventilation and spontaneous breathing was used, based on previous models (21,24). A bilateral thoracotomy was performed sequentially and varying standardized lung lesions were created in an explorative study design, after which AL was measured on both lungs after chest closure with a digital drainage system.

The sheep included in the analysis were used in three experiments, one *post-mortem* study and two *in vivo* studies. First, superficial parenchymal lung lesions were tested in mechanically ventilated *post-mortem* sheep (N=2 cadavers), to test the hypothesis that pleural apposition diminishes AL for superficial lesions after chest closure (27,28). Then, such lesions were created in a live sheep model (*in vivo*), testing their natural healing course in the presence of intact coagulation (N=3 sheep). Finally, based on the previous results, more extensive lesions involving macroscopically visible bronchioles were tested (N=7 sheep). Part of the lesions made in the *in vivo* studies were treated with a sealant. For the present study, we only pooled results for untreated lesions, as the focus of this investigation was to study the mechanisms of intrinsic sealing.

Lung lesions

Lesions were made to simulate the clinical problem of an alveolar-pleural fistula, defined as PAL arising distal to the segmental bronchus (29). Three different lung lesions were tested: superficial parenchymal, deep bowl-shaped and sequential lung amputation lesions. Superficial parenchymal lesions were made by creating $n \times n$ perpendicular cuts in a 25 mm × 25 mm square with a scalpel limited to 1–3 mm depth (*Figure 1A,1B*). Deep bowl-shaped lesions were made by cutting a ⌀25 mm bowl lesion using biopsy punches and scissors (*Figure 1C,1D*). Sequential lung amputations were made by cutting away tissue perpendicularly to the expected bronchiole branching pattern, at a width of 3–5 cm in steps of 1 cm until either bronchioles of >⌀1.5 or ⌀0.5 mm were encountered, on the ventral tips of the right middle lobe (RML) and right lower lobe (RLL) on the right, plus the left upper lobe (LUL) and the left lower lobe (LLL) on the left side (*Figure 1E,1F*). This method for inducing lesions involving bronchioles was found to be the most repeatable in our *ex vivo* investigations [Supplementary file (Appendix 1)] and is based on the model of Ranger (21). All lesions were made on a static lung with a positive end-expiratory pressure (PEEP) of 10 cmH_2O. Precise lesion types per experiment are explained in *Table 1*.

Outcome measures

In all experiments, after lesion creation and chest closure, AL was measured using a digital chest drainage system (Thopaz®, Medela, Baar, Switzerland). The time point since start of drainage when AL was <20 mL/min, was noted as time until intrinsic sealing. For lesions involving bronchioles, the AL was measured using a mechanical ventilator (SERVO-I®, Getinge, Gotenburg, Sweden), based on the inspiratory (TVi) and expiratory (TVe) tidal volumes, right before and after lesion induction. The minimal leaking pressure (MLP) was determined for these lesions by dialing down the PEEP in steps of 1 cmH_2O until leakage disappeared or increasing in steps of 1 cmH_2O until leakage appears. In the *in vivo* series, the *post-mortem* measurements of MLP were performed either *ex-situ* after lung explantation, or *in-situ* using selective intubation (in E4–E6, *Table 1*). Bronchial diameters (lumen, ⌀) were measured using a ruler with markings every 0.5 mm (Aesculap AA804R), and approximated in 0.5 mm increments. Finally, macroscopy was recorded descriptively, paying attention to mechanisms of sealing, hemostasis and atelectasis.

Animal procedures

All experiments were performed under a project license (No. AVD10300202114869) granted by national authorities ('Centrale Commissie Dierproeven', CCD) after review by an independent ethics board ('Dierexperimentencommissie', DEC) in the Netherlands, in compliance with institutional guidelines for the care and use of animals. Humane care and anesthesia were provided throughout the experiments. Experimental protocols were approved by the animal welfare body and registered internally at our institute (Nos. 2021-0012-001 and 2021-0012-002).

Adult mixed-breed female sheep (N=2) which were previously utilized for the production of antibodies in an unrelated project were euthanized using an overdose of

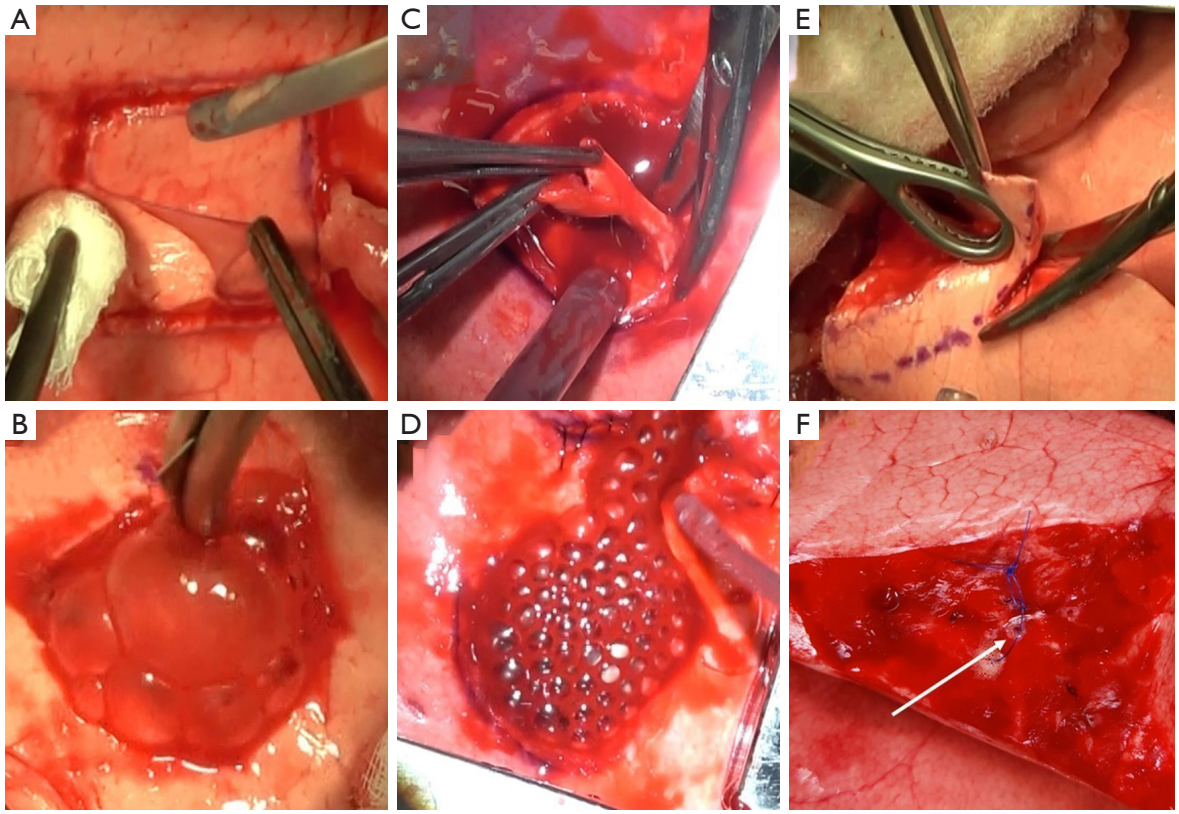

Figure 1 Lung lesions. (A,B) Superficial parenchymal lesion creation *in vivo*; (C,D) deep bowl-shaped lesion creation *in vivo*; (E,F) sequential lung amputation lesion *in vivo*. White arrow points at a macroscopically visible bronchiole (marked with a suture for recognition at obduction).

pentobarbital, and the cadavers were directly re-used in the *post-mortem* pilot model. Healthy adult mixed-breed female sheep (N=10) were used in the *in vivo* animal model. Anesthetic protocols *in vivo* involved deep surgical anesthesia during surgery and lighter sedation during a spontaneous ventilation observation period [detailed in Supplementary file (Appendix 1)]. Mechanical ventilation was guided by the visual presence of atelectasis on lung surfaces and ventilation and oxygenation requirements in the live animals. Reduction of ruminal tympany was ensured throughout the procedure.

A thoracotomy was performed on both sides of in the fifth intercostal space sequentially, always beginning with the right lung. After lesion creation, hemostasis was performed if required using gauzes and diathermy, and time until hemostasis was recorded. If necessary, fibrin plugs were removed using a small tweezers from the bronchiole lesions following hemostasis. Following all measurements, a silicone drainage tube (size Ch30) was placed apically and exited the thorax ventrally on both sides. The thoracotomy was closed in layers to ensure air-tightness for accurate AL measurements. After an observation period in a back position (*post-mortem* model, minimum of one hour) or abdominal position (*in vivo* model, minimum of three hours) under mechanical or spontaneous ventilation, the live animals were euthanized using pentobarbital. The lungs were explanted through a median sternotomy for inspection, *post-mortem* measurements and histology.

Histology

For histological analysis, samples were taken from the created defects after MLP determination and stored in 4% formaldehyde. Subsequently, they were embedded in paraffin and 4 µm thick sections were cut and stained with hematoxylin-eosin staining. These coupes were digitalized and assessed by an experienced pathologist (Vos S).

Table 1 Baseline characteristics of the experiments

ID	Weight, age	Mode of ventilation	Side	Tot. (n)	Eff. (n)	Type	Eff. lobe and lesion	Drainage duration (h)
Post-mortem								
T3	68.5 kg, 9 y 1 mo	MV: PC, Pmax 40 cmH_2O	L	1	1	*Par.*	LUL: 25 mm × 25 mm × 1 mm visceral pleura removal with 10×10 incisions at 1 mm depth	1:20
			R	1	1	*Par.*	RML: 25 mm × 25 mm × 3 mm cube excision	4:10
T4	75.5 kg, 6 y 4 mo	MV: PC, Pmax 50 cmH_2O	L	1	1	*Par.*	LUL: same as T3/L	1:20
			R	1	1	*Par.*	RLL: same as T3/L	3:30
In vivo								
P1	73 kg, 3 y 6 mo	MV: VC, Pmax 38 cmH_2O; SV: 2 h	L	1	1	*Par.*	LUL: same as T3/L + additional 10×10 incisions at 3 mm depth	3:10
			R	1	1	*Par.*	RLL: same as T3/L	7:40
P2	60.3 kg, 2 y 8 mo	MV: VC, Pmax 36 cmH_2O; SV: –	L	2	1	*Par.*	LUL: same as T3/L but 3 mm depth incisions	3:30
			R	2	1	*Br.*	RLL: ⌀25 mm/1 mm depth, 2× ⌀10 mm/5 mm depth, cut bowl + 10×10 incisions at 1 mm depth	7:40
P4	50 kg, 1 y 7 mo	MV: PC, Pmax 40 cmH_2O; SV: 4:30 h	L	5	1	*Par.*	LUL: same as T3/L but 6×6 incisions at 3 mm depth	5:10
			R	5	1	*Par.*	RML: same as T3/L but 6×6 incisions at 3 mm depth	8:00
P5	71 kg, 2 y 9 mo	MV: PC, Pmax 30 cmH_2O; SV: 3:00 h	L	2	2	*Br.*	LUL/LLL: sequential amputations until bronchioles of ⌀1.5 mm	3:10
			R	2	2	*Br.*	RML/RLL: same as P5/L	6:50
P6	67.5 kg, 2 y 10 mo	MV: PC, Pmax 40 cmH_2O; SV: –	L	2	2	*Br.*	LUL/LLL: sequential amputations until bronchioles of ⌀0.5 mm	–
			R	2	2	*Br.*	RML/LLL: same as P6/L	4:40
E2	82 kg, 2 y 11 mo	MV: PC, Pmax 25 cmH_2O; SV: 4:09 h	R	2	2	*Br.*	RML/RLL: same as P5/L	10:09
E3	79.8 kg, 1 y 2 mo	MV: PC, Pmax 25 cmH_2O; SV: 4:07 h	L	2	2	*Br.*	LUL/LLL: same as P5/L	4:33
E4	66.3 kg, 3 y 2 mo	MV: PC, Pmax 25 cmH_2O; SV: 3:24 h	R	1	1	*Br*	RLL: same as P5/L	7:08
E5	67 kg, 3 y 5 mo	MV: PC, Pmax 25 cmH_2O; SV: 3:01 h	L	1	1	*Br*	LLL: same as P5/L	3:27
E6	66 kg, 1 y 8 mo	MV: PC, Pmax 25 cmH_2O; SV: 3:08 h	L	1	1	*Br*	LLL: same as P5/L	3:45

ID, identifier; Tot., total lesions; Eff., effective number of lesions leaking on one side, other created lesions were sealed before thorax closure; y, years; mo, months; kg, kilograms; MV, mechanical ventilation; PC, pressure control; Pmax, maximum pressure; h, hours; VC, volume control; SV, spontaneous ventilation; L, left; R, right; Par., superficial parenchymal type lesions; Br., deeper lesions involving bronchioles; LUL, left upper lobe; RML, right middle lobe; RLL/LLL, right/left lower lobe.

Statistical analysis

ThopEasy + software (Medela, Baar, Switzerland) was used to import AL data, giving mean AL values (mL/min) every 10 minutes. For all lesions (*post-mortem* and *in vivo*), the mean AL was calculated over the first 80 minutes of drainage (minimum drainage time across all groups). *In vivo*, mean AL was calculated over the first 180 minutes of drainage, and in 30 minute intervals for the first 5 hours of drainage. For statistical comparison, drainage AL data was normalized as: $AL_{normalized} = \ln\left(\frac{AL}{N_{leaks}}\right)$, were N_{leaks} denotes the number of effective ALs on the drained side. Normalized values were then compared using an analysis of variance (ANOVA) with Bonferroni-Holm post-hoc test (α=0.05/3). Intraoperative AL (mL/min) based on the mechanical ventilator was calculated as: $AL = \left(\frac{\sum_{k=1}^{5}\left(TVi_k - TVe_k\right)}{5}\right) \times RR$, were RR denotes respiratory rate. This AL was corrected for AL measured before the lesion was created as: $AL_{corrected} = AL_{lesion} - AL_{baseline}$. In case this calculation resulted in a negative AL, an AL of 0 mL/min was noted. MLP, time until hemostasis and AL data were compared between lesions involving bronchioles (⌀0.5 mm *vs.* >⌀1.5 mm lesions) using a Mann-Whitney *U* test (two-tailed α=0.05). IBM SPSS Statistics 27 (IBM Corp., Armonk, New York, USA) was used for statistical testing.

Results

Summary of experiment characteristics

In twelve animals, 25 untreated lesions were created and analyzed (N=4 superficial parenchyma *post-mortem*, N=5 superficial parenchyma *in vivo*, N=16 lesions involving bronchioles, N=4 ⌀0.5 mm and N=11 >⌀1.5 mm bronchioles, N=1 missing diameter). One animal in the *in vivo* group (P2) did not regain spontaneous ventilation and was kept on the mechanical ventilator during the observation period, another (P6) died due to acute cardiac arrest right after closure of the left thoracotomy, resulting in missing left lung drainage data and a shorter follow-up period. All experiment characteristics are displayed in *Table 1*.

Air leak characteristics for lesion subtypes

75% of superficial parenchymal lesions resulted in AL after thorax closure in the *post-mortem* model [mean ± standard deviation (SD): 760±693 mL/min, N=4]. One lesion did not exhibit AL, likely due to extensive atelectasis of the affected lobe seen at obduction. For the *in vivo* superficial parenchymal lesions, only minimal and rapidly decreasing post-operative AL was observed (mean ± SD: 42±33 mL/min, N=5, *Figure 2A*). All of these lesions stopped leaking within a median time of 20 minutes [interquartile range (IQR), 10–75 minutes, N=5]. The average AL at 80 minutes showed a trend towards statistical significance between the *post-mortem* and *in vivo* groups (P=0.055).

In comparison to superficial parenchymal lesions *in vivo*, all lesions involving bronchioles (pooled ⌀0.5 mm and >⌀1.5 mm lesions) led to significantly higher AL post-operatively (normalized flow mean ± SD: 459±221 mL/min, P=0.003, N=9, *Figure 2A*,*2B*). Despite relevant AL initially, the magnitude of the AL still decreased over the observation period (*Figure 2C*). At termination of the experiment, 5/9 (55.6%) of these lungs were still leaking (median drain time: 273 minutes, IQR, 207–435 minutes, N=5), and intrinsic sealing for the remaining lungs occurred within a median of 115 minutes (IQR, 52–245 minutes, N=4). The shortest time until intrinsic sealing was observed for the lung affected with a ⌀0.5 mm bronchiole lesion (50 minutes, N=1).

Bronchiole diameter and leakage capabilities

Comparing both sizes of bronchioles, >⌀1.5 mm lesions (N=11) were found to require longer time until hemostasis then ⌀0.5 mm lesions (N=4) (mean ± SD: 6.0±2.7 *vs.* 2.0±0 minutes, P=0.012). However, no significant difference was found between >⌀1.5 mm/⌀0.5 mm lesions for MLP (median ± IQR, 5±2 *vs.* 7±5 cmH_2O, P=0.226) nor mechanical ventilator AL (median ± IQR, 581±1,012 *vs.* 140±305 mL/min, P=0.104) during the live observation. Furthermore, *post-mortem* MLP did not differ significantly between >⌀1.5 mm/⌀0.5 mm (median ± IQR, 6±13 *vs.* 10±41 cmH_2O, P=0.199) A trend was seen for higher AL alive and lower MLP *post-mortem* for the >⌀1.5 mm lesions. Of note, N=2 lesions were excluded from MLP analysis in the >⌀1.5 mm subgroup due to blood contact during obduction, which possibly influenced the MLP (15 and 45 cmH_2O).

Macroscopy and histology

A rapid intrinsic sealing of the *in vivo* superficial parenchymal lesions was observed intraoperatively (illustrated in

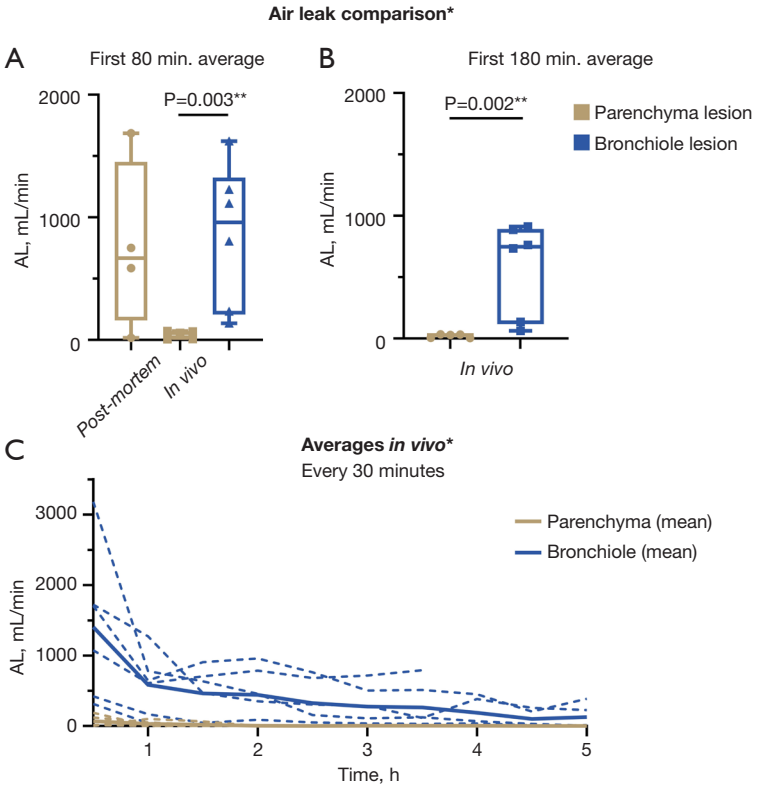

Figure 2 AL results for parenchymal and bronchiole lesions. (A) Average AL from first 80 minutes of thoracic drainage; (B) average AL from the first 180 minutes of thoracic drainage; (C) average AL values per 30 minutes from *in vivo* experiments. Dashed lines show individual drain measurements. *, absolute AL values for left or right drains, uncorrected for number of leaks per side (*Table 1*); **, statistical testing performed using ANOVA (α=0.05) on log-normalized AL values and Bonferroni-Holm correction for post-hoc testing (only significant comparisons shown). min., minutes; h, hours; AL, air leakage; ANOVA, analysis of variance.

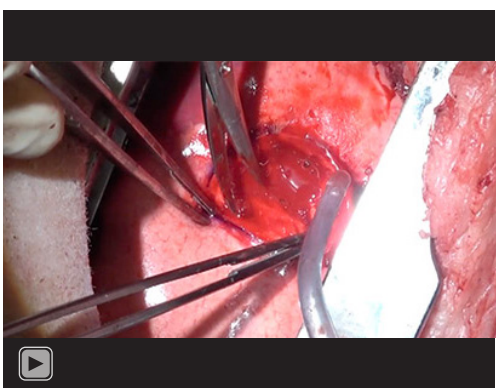

Video 1 Intraoperative footage of rapid intrinsic sealing mechanisms of parenchymal lesions.

Video 1). At obduction, all superficial parenchymal lesions of the *in vivo* model were covered with a coagulated fibrin sealing layer (*Figure 3A,3B*). For the lesions involving bronchioles, the bronchioles appeared contracted or were no longer macroscopically visible (*Figure 3C,3D*).

Histology for the superficial parenchymal lesions (N=2 lesions after <12 h) revealed an area of alveolar collapse surrounding the injured sites, extending beyond the coagulated parenchymal incisions. Within this area of alveolar collapse, intra-alveolar hemorrhage was observed. Going further proximally, the normal air contents of the parenchyma gradually returned. Minimal influx of immune cells was seen, but no notable immune response was

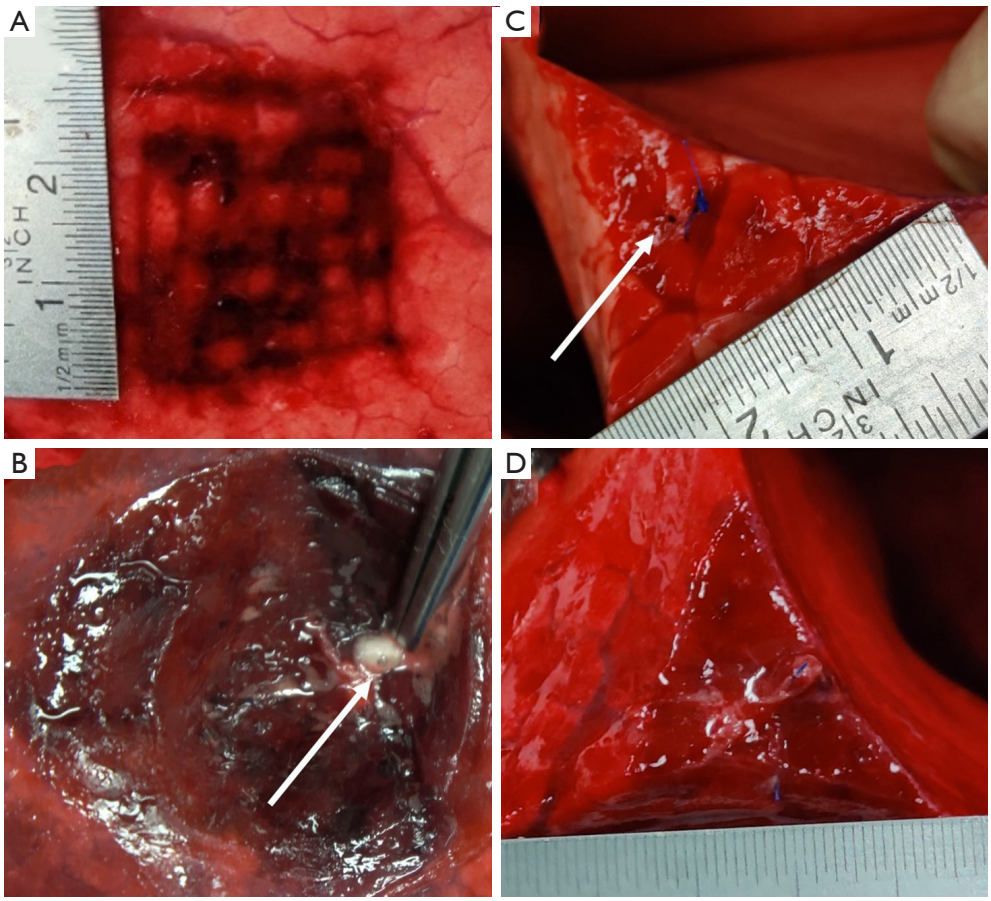

Figure 3 Macroscopic findings. (A) Intrinsically sealed superficial parenchymal lesion, with a coagulated fibrin layer over the lesion. (B) Small bronchiole (white arrow) as air leak focus of a deep bowl-shaped lesion with some secretions. Note the intrinsic sealing layer over the lung parenchyma. (C) Macroscopic aspect of sequential amputation *in vivo* and (D) the same lesion at obduction. Note that the bronchiole (white arrow) is no longer visible at obduction and that a coagulated sealing layer is present on top of the parenchyma.

noted (*Figure 4*). The histological response for the lesions involving bronchioles was similar to the parenchymal lesions *in vivo* [Supplementary file (Appendix 1), Figure S3].

Discussion

This study revealed that superficial parenchymal defects are unsuited for lung sealant testing in a healthy ovine model of PAL, due to rapid intrinsic sealing. Sequential amputation lesions involving bronchioles do result in AL in 56% of cases (median observation time: 4:33 h), but with 44% of cases sealing intrinsically in a median time of 1:55 h. Bronchioles of >⌀1.5 mm are preferable over ⌀0.5 mm, due to a trend towards a longer time to sealing. These lesions can be created in a reproducible manner and therefore seem valid for acute lung sealant testing. Nevertheless, the time to sealing is still too short for analysis of pPAL. These observed intrinsic sealing mechanisms could explain a translational gap in lung sealant research, especially in studies lacking negative control groups to demonstrate pPAL.

Comparison to literature

Presently, many clinical studies have been performed, testing numerous different sealant products. Some sealants were shown to be effective, but there were fluctuating results and no clear evidence based recommendations (16). As we suggest, disappointing results in clinical studies may be a consequence of a translational gap when negative controls are not used in the preclinical phase to ensure significant PAL. For example, effectiveness of fibrin glue was seen in an animal study that compared bursting pressures of fibrin glue

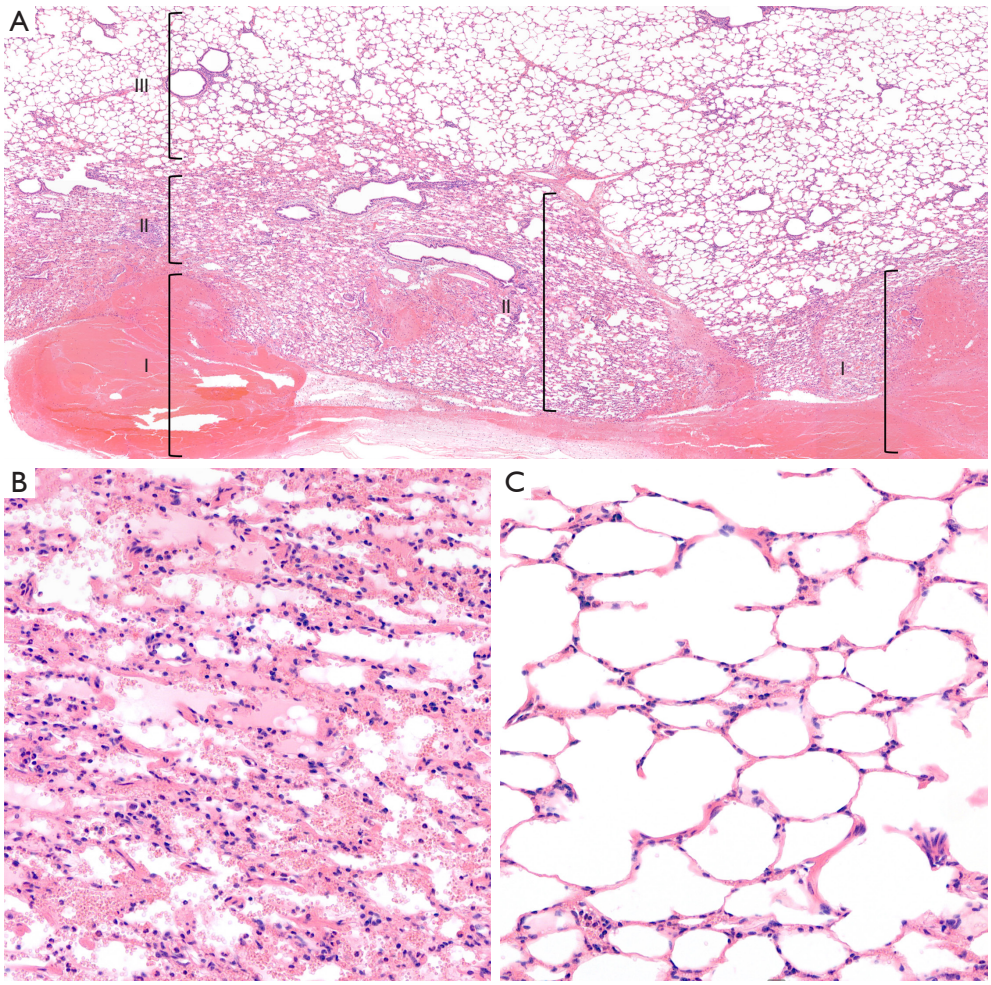

Figure 4 Histology of intrinsically sealed lung parenchyma. (A) Aspect of a 3 mm deep parenchymal incision (5× magnification). Three areas can be distinguished in the intrinsic sealing layer: area I shows coagulation in the incision itself; area II shows alveolar collapse and intra-alveolar hemorrhages extending beyond the actual incision site (detailed at 40× magnification in B) and area III shows the return of normal air containing alveoli. (C) Uninjured lung site shows normal air containing parenchyma (40× magnification). Hematoxylin-eosin staining.

with sutures in a rabbit model, without a negative control group (i.e., lesion with no treatment) (30). In contrast, the animal study by McCarthy *et al.*, which included a negative control group to demonstrate significant PAL, showed no real effect of fibrin glue. Fifty percent of the animals in their study were free of AL after 24 h in both the fibrin glue and negative control groups (i.e. similar effectiveness to natural healing) (24). This study is in line with clinical literature, as fibrin glue has not been found significantly effective for reducing the length of hospital stay in the clinical trials by Fleisher, Wong and Mouritzen (31-33).

Our study confirms the hypothesis that it is only possible to induce PAL in healthy animal lungs when creating lesions with adequate depth, lacerating terminal bronchiole (21). Previous studies with negative control groups had similar findings, as amputations of lung lobes or deep incisions, likely resulting in bronchiolar leaks, resulted in AL complications [Supplementary file (Appendix 1), Table S1] (21,34-36). As an example, Ranger *et al.* produced similar bronchiolar leaks of >⌀1.5 mm and found higher AL (mean 1.4 L/min, range 0.6–3.5 L/min) in small dogs with similar drainage settings, as compared to our finding. These differences may be explained by sampling variation or lobe/species effects (21). In contrast, various superficial lesions did not lead to AL problems (18,37-39). Also in larger parenchymal lesions, AL

may persist, although in small dogs and pigs (17–35 kg) it is unclear whether this is due to some degree of bronchiolar laceration at depths of ~5 mm (24,40).

Intrinsic sealing mechanisms

Pathologically, the intrinsic sealing layer is hypothesized to be more than just superficial coagulation, an extended area of alveolar collapse might be an explanation for the strong and rapid intrinsic sealing seen in this study. Similar mechanisms have previously been described, including compressed or partially aerated alveoli, subpleural alveolar edema, intra-alveolar bleeding and intra-alveolar deposition of fibrin strands (19,41-43). Based on these studies and the findings in our study, the following mechanisms are proposed to be principally responsible: first, alveolar collapse is physically initiated by air escaping from the subpleural alveolar layer, by direct impression of the surgical instrument and a lower resistance to flow of this distal AL path (41). Simultaneously, hemorrhage spreads through the pores of Kohn and channels of Lambert (43). Blood proteins and lipids are known to cause an inhibition of surfactant function, increasing alveolar surface tension (Laplace's law, $P=\frac{2T}{r}$) and thereby attenuating alveolar collapse biophysically (44-48). This results in a reduction of the common radius of the subpleural alveoli, increasing the resistance and reducing the AL by Poiseuille's law. This attenuates coagulation mechanisms analogous to vasoconstriction in a bleeding wound (41,43). Inflammatory mechanisms were not seen in our sample (due to the short follow-up period), but may further enhance sealing through alveolar compression, due to capillary enlargement and edema as previously described (19,42,43). Pleural apposition may also reduce AL, but we hypothesize this to play a small role based on our *post-mortem* observations and rapid sealing seen intra-operatively (27).

These micromechanics could also provide a biophysical explanation for the lower intrinsic sealing capabilities in diseased human lungs. Pulmonary emphysema is a major risk factor for pPAL, and emphysema scores have shown to be predictive of pPAL (1,49-51). Conceptually, in emphysematous lungs, lower pressures are required to prevent alveolar collapse, due to the larger radius of emphysematous alveoli (Laplace's law). Therefore, it is hypothesized that the proposed biophysical intrinsic sealing mechanisms will not induce the same degree of intrinsic sealing by alveolar collapse as seen in the healthy, non-emphysematous ovine lungs. Further study of intrinsic sealing mechanisms in emphysematous lungs might help us understand mechanisms of pPAL, which may improve treatment of these lesions.

The reduction in bronchiole diameter which was observed macroscopically *post-mortem*, may be due to sympathetic nervous system activation or bronchiole collapse due to absence of hyaline cartilage supporting structures. Especially bronchioles <1 mm lack supporting hyaline cartilage, which was also seen histologically in our study [Supplementary file (Appendix 1), Figure S3] (52). In this case, as surrounding alveolar tissues collapse due to a steal phenomenon from the leaking orifice, especially bronchioles without cartilage support could collapse and seal intrinsically (as shown in *Figure 3D*). A bronchiole of >⌀1.5 mm appears preferable over ⌀0.5 mm to prevent rapid and strong intrinsic sealing in the acute aerostasis model from this perspective (21).

There might be species specific considerations for sheep, which explain the strong and rapid intrinsic sealing. These include intra-vascular macrophages and an increased white blood cell count, which may cause immune mediated attenuation of intrinsic sealing mechanisms (53-55). Coagulation times are comparable to those of humans (55). High doses of intravenous propofol (dissolved in lipids) were sometimes required during surgical anesthesia, and it was hypothesized that this might result in hyperlipidemia and subsequently increased blood viscosity and coagulability. However, previous *in vitro* and *in vivo* experiments have shown no effect on blood viscosity, and even describe a reduced platelet aggregation (56).

Translational value of air leak models

The face validity of a bronchiolar AL model is reduced, as clinical pPAL mostly arises from the alveoli in superficial parenchymal injury, such as from the dissection of fissures or pleural adhesions. As an acute aerostasis model, the construct validity remains preserved. PAL >500 mL/min intraoperatively was found to predict pPAL, and AL sizes of 150–400 mL/min have been used for sealant application in a clinical trial, with positive results (57,58). Thus, the bronchiole AL seems sufficient for acute sealant testing. The model allows testing on an actively leaking lung, after thoracic closure, at least before intrinsic sealing of specific bronchiole lesion occurs. Thereby, other important mechanisms such as coagulation, immune response, pleural mechanisms and physiological breathing can be replicated, which is presently not feasible in animal-free

alternatives (59,60).

Disease models may be suitable to induce pPAL, but it remains unclear how long PAL should last in a model for sealant testing. Based on the hypothesized micromechanics, emphysema may result in longer pPAL, while heparinization seems a less effective disease model, as this would not inhibit alveolar collapse, and might even enhance spreading of blood through the alveoli. One study found significantly lower bursting pressures for sealants applied to emphysematous lungs, but did not measure PAL postoperatively (26). The lower bursting pressures could be biochemically ascribed to a lower crosslink density on emphysematous lungs, which may be another explanation for a translational gap (26). When developing disease models, disease induction might be associated with an increased baseline variation, higher sample size requirement and decreased animal welfare, which needs to be weighed against the potential added benefit of these models.

Limitations

These experiments offer a valuable addition to the present preclinical literature, by confirming the possibility of a translational gap and offering novel insights into intrinsic sealing mechanisms. However, based on these experiments, it is not possible to define a global standardized model for pPAL and lung sealant research. For this, further investigations are needed. First of all, it needs to be studied how long PAL needs to be present in a model for sealant testing to ensure accurate translation. Formulated differently, the time until intrinsic sealing of human lungs when a sealant is applied needs to be studied. Disease models are hypothesized to be suitable options for developing longer leaking PAL, but remain entirely unconfirmed, and come with added costs (higher sample size, decreased animal welfare). Another option might be to create leaks in large bronchi (e.g., segmental bronchi), but this further decreases the face validity. Finally, due to small sample size and heterogenous methods in the present study, all findings described here should be interpreted with appropriate caution and need to be confirmed in *a-priori* statistically powered experiments.

Recommendations for further research

Clinicians and experimental researchers should be aware of the intrinsic sealing mechanisms of healthy animal lungs. Success of sealants in animal studies should therefore be interpreted cautiously. In new experimental design, negative control groups should always be considered to measure the actual treatment effect. PAL may be created in animal models by creating especially large defects or lacerating bronchioles of >ø1.5 mm (21,24). For development of a global standardized pPAL model, further research is required into the requirements of valid pPAL models (e.g., duration of PAL), and methods for inducing longer PAL (e.g., emphysema or heparinization) (25,26). Such disease models could also be used to study mechanisms of PAL in clinical scenario's, such PAL arising from stapler lines. The understanding of PAL sealing mechanisms is still incomplete, and the proposed mechanisms should be further investigated. With a thorough understanding hereof, a clinical solution for the problem of pPAL might be discovered, for example by making the surgical treatment better synergize with the underlying mechanisms of the specific lesion type. The conduction of animal systematic reviews and adherence to ARRIVE guidelines should be encouraged to further improve scientific rigorousness of animal studies (20,61).

Conclusions

Superficial parenchymal lesions exhibit an intrinsic sealing mechanism in a healthy ovine lung model, explained pathologically by an extended area of alveolar collapse attenuating coagulation mechanisms. These mechanisms may reduce model validity and contribute to a translational gap in lung sealant research, especially when negative control groups are not used. Experimental researchers should account for these mechanisms when designing experiments, to improve clinical applicability. One such approach for acute lung sealant testing in an ovine model, is to create deep parenchymal defects involving at least bronchioles of >ø1.5 mm. Further study into PAL models is required to develop and validate a universal standardized acute aerostasis model.

Acknowledgments

The authors would like to thank Nicole Calon, Jort Evers, Alex Hanssen, Stefanie Schönfeld, Maikel School and Pim van Sambeeck (all are affiliated with the Radboud University Medical Center in Nijmegen, The Netherlands) for their help during the experiments, Pieter Verbost and Manon van Hulzen for their help with the experimental protocols and licenses and all other supporting personnel in the animal laboratory for their great caretaking of all laboratory animals.

We want to thank the Radboudumc Department of Statistics for its help with the statistical analysis and the Department of Pathology for helping with processing the histological samples. Part of this work has previously been presented at the SEOHS 2022 conference in the Netherlands. Finally, we thank Willem de Boode for help with conceptual understanding of the intrinsic sealing mechanism.
Funding: This work was supported by GATT Technologies B.V. (Nijmegen, The Netherlands).

Footnote

Reporting Checklist: The authors have completed the ARRIVE reporting checklist. Available at https://jtd.amegroups.com/article/view/10.21037/jtd-23-180/rc

Data Sharing Statement: Available at https://jtd.amegroups.com/article/view/10.21037/jtd-23-180/dss

Peer Review File: Available at https://jtd.amegroups.com/article/view/10.21037/jtd-23-180/prf

Conflicts of Interest: All authors have completed the ICMJE uniform disclosure form (available at https://jtd.amegroups.com/article/view/10.21037/jtd-23-180/coif). EAR is an employee of GATT Technologies B.V. and HvG was a scientific advisor for GATT Technologies B.V. until 31 December 2021, but not in relation to lung sealing technology. BPH received funding and study materials through the institution for conduction of the study from GATT Technologies B.V. The other authors have no conflicts of interest to declare.

Ethical Statement: The authors are accountable for all aspects of the work in ensuring that questions related to the accuracy or integrity of any part of the work are appropriately investigated and resolved. All experiments were performed under a project license (No. AVD10300202114869) granted by national authorities ('Centrale Commissie Dierproeven', CCD) after review by an independent ethics board ('Dierexperimentencommissie', DEC) in the Netherlands, in compliance with institutional guidelines for the care and use of animals. Humane care and anesthesia were provided throughout the experiments. Experimental protocols were approved by the animal welfare body and registered internally at our institute (Nos. 2021-0012-001 and 2021-0012-002).

References

1. Attaar A, Tam V, Nason KS. Risk Factors for Prolonged Air Leak After Pulmonary Resection: A Systematic Review and Meta-analysis. Ann Surg 2020;271:834-44.
2. Attaar A, Luketich JD, Schuchert MJ, et al. Prolonged Air Leak After Pulmonary Resection Increases Risk of Noncardiac Complications, Readmission, and Delayed Hospital Discharge: A Propensity Score-adjusted Analysis. Ann Surg 2021;273:163-72.
3. Brunelli A, Xiume F, Al Refai M, et al. Air leaks after lobectomy increase the risk of empyema but not of cardiopulmonary complications: a case-matched analysis. Chest 2006;130:1150-6.
4. Liang S, Ivanovic J, Gilbert S, et al. Quantifying the incidence and impact of postoperative prolonged alveolar air leak after pulmonary resection. J Thorac Cardiovasc Surg 2013;145:948-54.
5. Yoo A, Ghosh SK, Danker W, et al. Burden of air leak complications in thoracic surgery estimated using a national hospital billing database. Clinicoecon Outcomes Res 2017;9:373-83.
6. Singhal S, Ferraris VA, Bridges CR, et al. Management of alveolar air leaks after pulmonary resection. Ann Thorac Surg 2010;89:1327-35.
7. Okereke I, Murthy SC, Alster JM, et al. Characterization and importance of air leak after lobectomy. Ann Thorac Surg 2005;79:1167-73.
8. Zaraca F, Brunelli A, Pipitone MD, et al. A Delphi Consensus report from the "Prolonged Air Leak: A Survey" study group on prevention and management of postoperative air leaks after minimally invasive anatomical resections. Eur J Cardiothorac Surg 2022;62:ezac211.
9. Kobayashi H, Sekine T, Nakamura T, et al. In vivo evaluation of a new sealant material on a rat lung air leak model. J Biomed Mater Res 2001;58:658-65.
10. Yanagihara T, Maki N, Wijesinghe AI, et al. Efficacy of

Alaska Pollock Gelatin Sealant for Pulmonary Air Leakage in Porcine Models. Ann Thorac Surg 2022;113:1641-7.
11. Belda-Sanchís J, Serra-Mitjans M, Iglesias Sentis M, et al. Surgical sealant for preventing air leaks after pulmonary resections in patients with lung cancer. Cochrane Database Syst Rev 2010;2010:CD003051.
12. Singhal S, Shrager JB. Should buttresses and sealants be used to manage pulmonary parenchymal air leaks? J Thorac Cardiovasc Surg 2010;140:1220-5.
13. Zhou J, Lyu M, Pang L, et al. Efficiency and safety of TachoSil® in the treatment of postoperative air leakage following pulmonary surgery: a meta-analysis of randomized controlled trials. Jpn J Clin Oncol 2019;49:862-9.
14. McGuire AL, Yee J. Clinical outcomes of polymeric sealant use in pulmonary resection: a systematic review and meta-analysis of randomized controlled trials. J Thorac Dis 2018;10:S3728-39.
15. Malapert G, Hanna HA, Pages PB, et al. Surgical sealant for the prevention of prolonged air leak after lung resection: meta-analysis. Ann Thorac Surg 2010;90:1779-85.
16. Aprile V, Bacchin D, Calabrò F, et al. Intraoperative prevention and conservative management of postoperative prolonged air leak after lung resection: a systematic review. J Thorac Dis 2023;15:878-92.
17. Brunelli A, Bölükbas S, Falcoz PE, et al. Exploring consensus for the optimal sealant use to prevent air leak following lung surgery: a modified Delphi survey from The European Society of Thoracic Surgeons. Eur J Cardiothorac Surg 2021;59:1265-71.
18. Poticha SM, Macaladad F, Lewis FJ. The control of air leaks following subsegmental pulmonary resections. Surg Gynecol Obstet 1965;120:803-9.
19. Kausel HW, LIndskog GE. The healing of raw lung surfaces after experimental segmental resection. J Thorac Surg 1955;29:197-211.
20. Hermans BP, Poos SEM, van Dort DIM, et al. Evaluating and developing sealants for the prevention of pulmonary air leakage: A systematic review of animal models. Lab Anim 2023. [Epub ahead of print]. doi: 10.1177/00236772231164873.
21. Ranger WR, Halpin D, Sawhney AS, et al. Pneumostasis of experimental air leaks with a new photopolymerized synthetic tissue sealant. Am Surg 1997;63:788-95.
22. Annabi N, Zhang YN, Assmann A, et al. Engineering a highly elastic human protein-based sealant for surgical applications. Sci Transl Med 2017;9:eaai7466.
23. Elvin CM, Vuocolo T, Brownlee AG, et al. A highly elastic tissue sealant based on photopolymerised gelatin. Biomaterials 2010;31:8323-31.
24. McCarthy PM, Trastek VF, Bell DG, et al. The effectiveness of fibrin glue sealant for reducing experimental pulmonary ari leak. Ann Thorac Surg 1988;45:203-5.
25. Balakrishnan B, Payanam U, Laurent A, et al. Efficacy evaluation of anin situforming tissue adhesive hydrogel as sealant for lung and vascular injury. Biomed Mater 2021.
26. Gika M, Kawamura M, Izumi Y, et al. The short-term efficacy of fibrin glue combined with absorptive sheet material in visceral pleural defect repair. Interact Cardiovasc Thorac Surg 2007;6:12-5.
27. Pedersen TB, Honge JL, Pilegaard HK, et al. Comparative study of lung sealants in a porcine ex vivo model. Ann Thorac Surg 2012;94:234-40.
28. Mentzer SJ, Tsuda A, Loring SH. Pleural mechanics and the pathophysiology of air leaks. J Thorac Cardiovasc Surg 2018;155:2182-9.
29. Clark JM, Cooke DT, Brown LM. Management of Complications After Lung Resection: Prolonged Air Leak and Bronchopleural Fistula. Thorac Surg Clin 2020;30:347-58.
30. Bergsland J, Kalmbach T, Balu D, et al. Fibrin seal--an alternative to suture repair in experimental pulmonary surgery. J Surg Res 1986;40:340-5.
31. Wong K, Goldstraw P. Effect of fibrin glue in the reduction of postthoracotomy alveolar air leak. Ann Thorac Surg 1997;64:979-81.
32. Mouritzen C, Drömer M, Keinecke HO. The effect of fibrin glueing to seal bronchial and alveolar leakages after pulmonary resections and decortications. Eur J Cardiothorac Surg 1993;7:75-80.
33. Fleisher AG, Evans KG, Nelems B, et al. Effect of routine fibrin glue use on the duration of air leaks after lobectomy. Ann Thorac Surg 1990;49:133-4.
34. Wilder RJ, Playforth H, Bryant M, et al. The use of plastic adhesive in pulmonary surgery. J Thorac Cardiovasc Surg 1963;46:576-88.
35. Nuchprayoon C, Tamayo AG, Reimann AF, et al. The use and tissue reaction of a biologic adhesive in the prevention of air leak following a transection of the lung. Dis Chest 1968;53:445-52.
36. Kanzaki M, Yamato M, Yang J, et al. Dynamic sealing of lung air leaks by the transplantation of tissue engineered cell sheets. Biomaterials 2007;28:4294-302.
37. Feito BA, Rath AM, Longchampt E, et al. Experimental

study on the in vivo behaviour of a new collagen glue in lung surgery. Eur J Cardiothorac Surg 2000;17:8-13.
38. Getman V, Devyatko E, Wolner E, et al. Fleece bound sealing prevents pleural adhesions. Interact Cardiovasc Thorac Surg 2006;5:243-6.
39. Büyükkale S, Çıtak N, İşgörücü Ö, et al. The effect of sodium hyaluronate-carboxymethyl cellulose membrane in the prevention of parenchymal air leaks: an experimental and manometric study in rats. Tuberk Toraks 2017;65:265-70.
40. Luh SP, Chou HH, Tsai TP, et al. Effect of Surgecel coverage with topical electrocauterization for preventing and sealing pulmonary air leakage. Int Surg 2004;89:190-4.
41. Joannides M, Hesse AL, Joannides M Jr. Surgical wounds of the lung; the mode of healing of pulmonary tissue. J Thorac Surg 1949;18:695-706.
42. Findlay CW Jr. The healing of surgical wounds of the lung with particular reference to segmental lobectomy. J Thorac Surg 1950;20:823-34.
43. Wheeldon EB, Mariassy AT, McSporran KD. The pleura: a combined light microscopic and scanning and transmission electron microscopic study in the sheep. II. Response to injury. Exp Lung Res 1983;5:125-40.
44. Zuo YY, Veldhuizen RA, Neumann AW, et al. Current perspectives in pulmonary surfactant--inhibition, enhancement and evaluation. Biochim Biophys Acta 2008;1778:1947-77.
45. Raghavendran K, Willson D, Notter RH. Surfactant therapy for acute lung injury and acute respiratory distress syndrome. Crit Care Clin 2011;27:525-59.
46. Holm BA, Keicher L, Liu MY, et al. Inhibition of pulmonary surfactant function by phospholipases. J Appl Physiol (1985) 1991;71:317-21.
47. Holm BA, Wang Z, Notter RH. Multiple mechanisms of lung surfactant inhibition. Pediatr Res 1999;46:85-93.
48. Walter F. Boron ELB. Medical Physiology Medical Physiology 3rd edition ed. Philadelphia: Elsevier; 2017.
49. DeCamp MM, Blackstone EH, Naunheim KS, et al. Patient and surgical factors influencing air leak after lung volume reduction surgery: lessons learned from the National Emphysema Treatment Trial. Ann Thorac Surg 2006;82:197-206; discussion 206-7.
50. Moon DH, Park CH, Kang DY, et al. Significance of the lobe-specific emphysema index to predict prolonged air leak after anatomical segmentectomy. PLoS One 2019;14:e0224519.
51. Murakami J, Ueda K, Tanaka T, et al. Grading of Emphysema Is Indispensable for Predicting Prolonged Air Leak After Lung Lobectomy. Ann Thorac Surg 2018;105:1031-7.
52. Ball M, Hossain M, Padalia D. Anatomy, Airway. StatPearls. Treasure Island (FL): StatPearls Publishing Copyright © 2022, StatPearls Publishing LLC.; 2022.
53. Delano ML, Mischler SA, Underwood WJ. Biology and Diseases of Ruminants: Sheep, Goats, and Cattle. Laboratory Animal Medicine 2002:519-614. doi: 10.1016/B978-012263951-7/50017-X.
54. Matute-Bello G, Frevert CW, Martin TR. Animal models of acute lung injury. Am J Physiol Lung Cell Mol Physiol 2008;295:L379-99.
55. Wilhelmi MH, Tiede A, Teebken OE, et al. Ovine blood: establishment of a list of reference values relevant for blood coagulation in sheep. ASAIO J 2012;58:79-82.
56. Reinhart WH, Felix Ch. Influence of propofol on erythrocyte morphology, blood viscosity and platelet function. Clin Hemorheol Microcirc 2003;29:33-40.
57. Brunelli A, Salati M, Pompili C, et al. Intraoperative air leak measured after lobectomy is associated with postoperative duration of air leak. Eur J Cardiothorac Surg 2017;52:963-8.
58. Zaraca F, Vaccarili M, Zaccagna G, et al. Cost-effectiveness analysis of sealant impact in management of moderate intraoperative alveolar air leaks during video-assisted thoracoscopic surgery lobectomy: a multicentre randomised controlled trial. J Thorac Dis 2017;9:5230-8.
59. Klassen C, Eckert CE, Wong J, et al. Ex Vivo Modeling of Perioperative Air Leaks in Porcine Lungs. IEEE Trans Biomed Eng 2018;65:2827-36.
60. Horvath MA, Hu L, Mueller T, et al. An organosynthetic soft robotic respiratory simulator. APL Bioeng 2020;4:026108.
61. Percie du Sert N, Hurst V, Ahluwalia A, et al. The ARRIVE guidelines 2.0: Updated guidelines for reporting animal research. PLoS Biol 2020;18:e3000410.

Cite this article as: Hermans BP, Li WWL, Roozen EA, van Dort DIM, Vos S, van der Heide SM, van der Heijden EHFM, ten Broek RPG, van Goor H, Verhagen AFTM. Intrinsic pulmonary sealing, its mechanisms and impact on validity and translational value of lung sealant studies: a pooled analysis of animal studies. J Thorac Dis 2023;15(9):4703-4716. doi: 10.21037/jtd-23-180

Appendix 1

Ex vivo characterization of sequential amputation lesions

Study setup

Using an *ex vivo* setup with ovine lungs, the repeatability of sequential lung edge amputations or lung incisions for attaining bronchioles of ≥1.5 mm but lower than 3.0 mm was investigated (same inclusion criteria as the model used by Ranger *et al.* in 1997). Next, the defect which was found most optimal was investigated in an *in vivo* acute aerostasis experiment and the intrinsic sealing capabilities were tested, by measuring minimal leaking pressures (MLP) at obduction and air leakage using a digital drain (see main manuscript).

Outcome measures

Bronchial diameters (lumen) were measured using a ruler with markings every 0.5 mm (Aesculap AA804R), and approximated in 0.5 mm increments. Bronchioles <0.5 mm but approximately larger than 0.25 mm were noted as 0.5 mm. If the bronchial lumen was approximately smaller than 0.25 mm or if no bronchiole lumen could be identified macroscopically, this was noted as 0 mm. MLP was determined using a Servo-I mechanical ventilator (Maquet critical care). Under pressure control settings, positive end-expiratory pressure (PEEP) was put on 10 cmH_2O while air leakage was assessed using water immersion or dripping water over the lesion. PEEP was gradually dialed down in steps of 1 cmH_2O until air leakage disappeared and the last plateau ventilatory pressure (Pplat) at which air leakage was still present was noted as MLP. In the case of MLP >10 cmH_2O, the pressure was gradually increased until leakage was observed. The dimensions (length and width) of sequential amputation lesions were measured in whole millimeters (Figure S1).

Sequential amputations versus incisional defects

First, two methods for attaining bronchiole lesions were compared *ex vivo*: sequential amputations versus lung incisions. For this, lungs of two sheep (54 and 84 kg) sacrificed for a different experiment were harvested immediately after death. Sequential lung amputations perpendicular to bronchial branching were compared with lung incisions regarding repeatability and leaking capability. Right upper (RUL), right middle (RML), right lower (RLL), left upper (LUL) and left lower lobes (LLL) were selectively intubated and fully recruited until Pmax =40–50 cmH_2O. All lesions were marked and created on a static lung with PEEP =10 cmH_2O. First, sequential amputations (*Figure S1*) were performed starting at 1 cm from the edge and measuring maximum bronchiole diameter and MLP during each increment until bronchioles of ≥1.5 mm were encountered. Then, a large clamp was placed across the defective area and the procedures were repeated on the same lobe for incisional defects (25 mm long, 5 mm deep and increasing depth in steps of 5 mm).

On the two lung specimens, a total of N=31 variations of the sequential amputation defect (N=10 1 cm from edge, N=10 2 cm from edge, N=7 3 cm from edge and N=4 4 cm from edge) and N=34 variations of the incision defect (N=10 at 5 mm depth, N=9 at 10 mm depth, N=10 at 15 mm depth, N=4 at 20 mm depth and N=1 at 30 mm depth) were created, N=2 for each RUL, RML, RLL, LUL and LLL. For the sequential amputations, a significant strong positive correlation was found between distance from the edge (1–4 cm) and maximum bronchiole diameter in the defect (Pearson correlation coefficient =0.635, P<0.001). This was also the case for incisional defects between incisional depth (5–30 mm) and maximum bronchiole diameter (Pearson correlation coefficient =0.678, P<0.001). However, the incisional defect produced outliers in maximum bronchiole diameter of 3–5 mm, while the sequential amputations showed a more predictable pattern of bronchiole diameter increase upon further amputations. In both cases, the maximum bronchiolar diameter showed a significant strong negative correlation with the MLP. For sequential amputations, the Pearson correlation coefficient was –0.739 (P<0.001) and for incisional defects –0.678 (P<0.001). These relations are shown visually in Figure S2. Based on this experimental data, it was decided that sequential amputation lesions will result in a more repeatable model regarding bronchiole diameters, and this defect was used in the following experiments. The RUL was no longer considered for further experiments, due to limited access and to increase comparability between right and left lung lesions *in vivo* (RML/LUL and RLL/LLL lesions are more comparable regarding their geometry).

https://dx.doi.org/10.21037/jtd-23-180

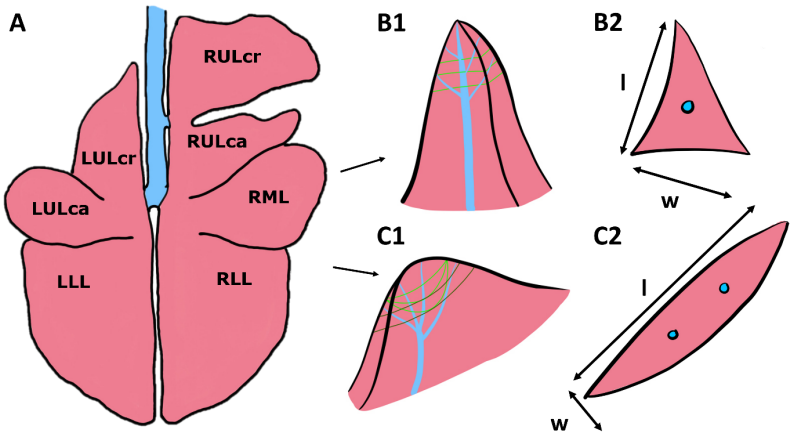

Figure S1 Schematic overview of lesion geometry. (A) Sequential amputation lesions are best performed on the RML/LULca/LLL/RLL in the *in vivo* situation, and are roughly made perpendicular to bronchial branching. (B1) Lesions on the RML/LULca are performed by sequentially increasing the cut line with 1 cm from the previous cut line (green lines), resulting in a triangular defect (B2). (C1) Lesions on the RLL/LLL are performed by increasing the cut depth, but limiting the cut width to allow for future patch placement in the model (light green lines, corresponds to the maximum defect width of 5 cm). This results in a roughly oval shaped defect (C2). In the initial *ex vivo* characterization experiment, the dark green cut lines were followed, leading to increased defect lengths.

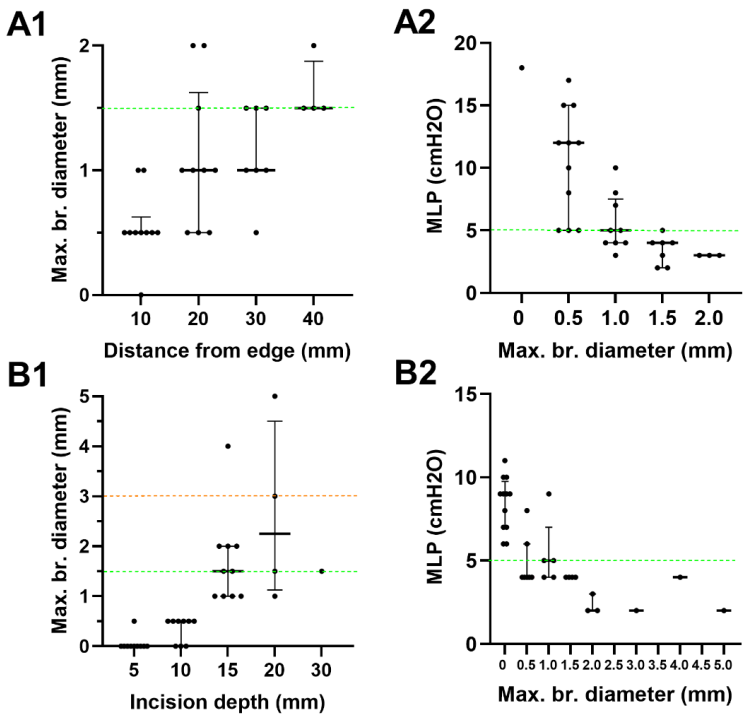

Figure S2 Sequential amputations versus incisional defects characterization. (A1) Sequential amputations defect shows a positive correlation between cut distance from edge, which follows a roughly linear and predictable pattern. From 2 cm distance from edge on, the 1.5 mm threshold for a suited model is passed (green line). (A2,B2) The bronchiole diameter in the defect is negatively correlated with the MLP. From 1.5 mm on, the MLP is consistently 5 cmH_2O or lower (green line). (B1) Incisional defect show a positive correlation with the incision depth, cut following a less predictable pattern. As can be seen, from 15 mm depth on, the 1.5 mm threshold for bronchial diameter is passed (green line), but the 3.0 mm upper limit (orange line) may also be exceeded.

https://dx.doi.org/10.21037/jtd-23-180

Anesthesia protocol in vivo studies

Housing remarks

Animals were transported to the research facility from a farm one day before the experiment together with two buddy sheep. Housing was in accordance with institutional protocols, and animals were fed ad-libitum up until the surgery.

Anesthesia

In these model development studies, anesthetic protocols were being optimized for the acute aerostasis model, which lead to some heterogeneity in used methods. P1 and P2 were pre-medicated using midazolam and carprofen, followed by induction of anesthesia using propofol in the jugular vein. P4, P5, P6, E2 and E3–E6 were pre-medicated using midazolam, ketamine and carprofen and anesthesia was induced using remifentanil and propofol through an intra-venous canula. They were then intubated and put on isoflurane during shaving and placement of a urinary catheter. Mechanical ventilator settings were adjusted based on the ventilation and oxygenation requirements. Propofol and remifentanil titrated for adequate blood pressure regulation (target mean arterial blood pressure during surgery: 50–100 mmHg) were used for anesthetic maintenance during surgery in P1 and P4, P5, P6, E2 and E3–E6, and propofol and sufentanil in P2. In P2, propofol was swapped out for pentobarbital halfway through the surgery to achieve a more stable blood pressure. Additionally, an arterial blood pressure line and ventilation line in the rumen (through a small epigastric incision in P1 and P2 and trans-esophageal in the remaining) were placed. The first sheep (P1) received a percutaneous tracheotomy canula to facilitate insertion of an endo-bronchial blocker (EZ-blocker) for single-lung procedures. Intermitted hyperoxygenation followed by apnea to facilitate defect creation on the lung was utilized for P2 and P4, P5, P6, E2 and E3–E6 as a less complicated alternative. An intercostal block was placed in all animals at three levels with a combination of lidocaine and bupivacaine. After surgery, the sheep were placed in an abdominal position, buprenorphine was administered and ketamine and midazolam were infused continuously to allow the sheep to breath spontaneously while still under anesthesia, and propofol was administered if required to maintain a deep anesthetic plane. During this spontaneous observation period, the animal was continuously monitored by an experienced biotechnician. Anesthetic monitoring throughout the procedure included end-tidal CO_2, oxygen saturation, pulse, blood pressure, arterial blood gasses and reflexes. At the end of the experiment, the sheep was euthanized by an overdose of pentobarbital.

https://dx.doi.org/10.21037/jtd-23-180

Histology of bronchiolar lesions

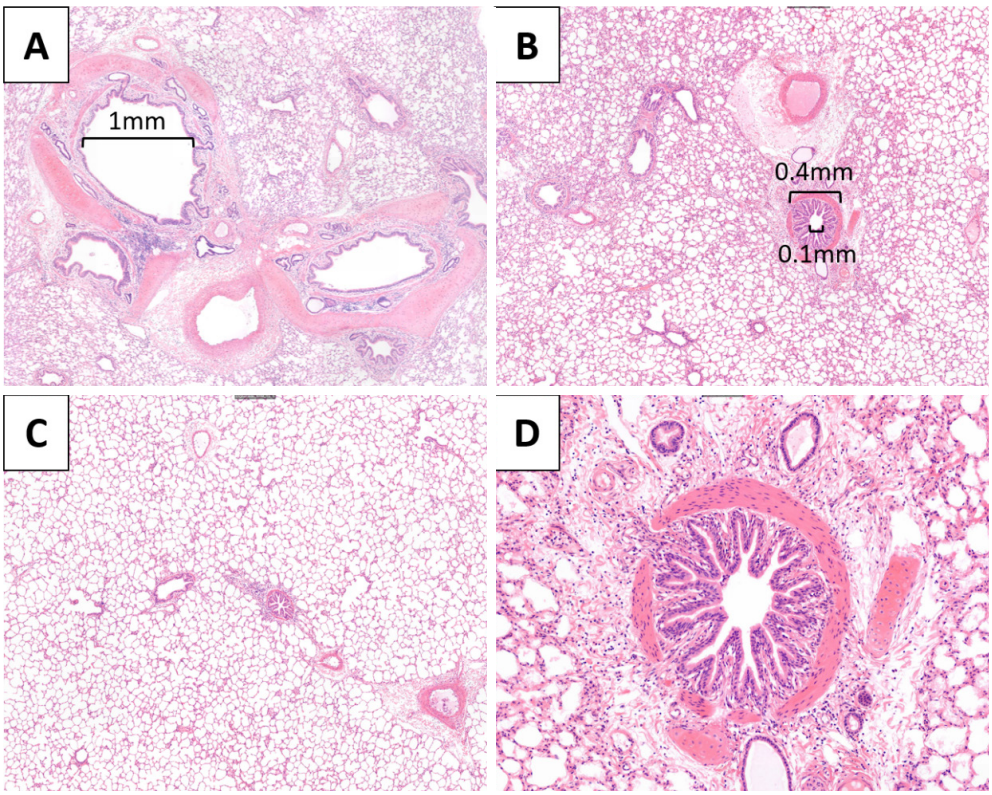

Figure S3 Histology of lesions including bronchioli. (A) Large bronchi are noted in this section, corresponding to macroscopic bronchi of ⌀1.5 mm. Note the hyaline cartilage around the lumen. Compared to normal parenchyma (C, control section), the alveoli in this section appear less aerated due to intra-alveolar bleeding and alveolar collapse. (B) Small bronchioles are seen, which appear contracted, and only a very small part of hyaline cartilage is seen (detail in D). However, the bronchioles in the normal parenchyma also have this similar contracted appearance (C). H&E staining: A, 1.6×; B, 2×; C, 2×; D, 5×.

https://dx.doi.org/10.21037/jtd-23-180

Literature table of previous animal studies with negative control groups

Table S1 Intrinsic sealing mechanisms from untreated pulmonary parenchymal lesions described in previously literature (based on comprehensive literature survey)

Author, year	Species, N	Lesion	Intrinsic sealing findings	Histology (intrinsic sealing)
Joannides, 1949 (41)	Dogs[a], ND	Crushing, punctures, tears, incisions, wedges, resection of lung tissue	Secretion plugging bronchioles. Alveolar compression due to air leak collapsing the lung after injury or after gentle compression[b]	Extended intra-alveolar bleeding. Compressed alveoli
Findlay, 1950 (42)	Cats, ND	Segmental lobectomy, residual parenchymal defect 2×1.5×1.5 cm. Middle lobe tip amputated and rotated into wound	Minimal air leak or pneumothorax. One animal died from BPF	Partial aeration of alveoli. Widening of the septa. Inflammatory response. Intra-alveolar blood
Kausel, 1955 (19)	Dogs, N=8	Segmental lobectomy, residual parenchymal defect 9–15 cm^2	No pneumothorax or air leaks. One animal died from BPF	Compressed alveoli. Intra-alveolar bleeding. Massive capillary enlargement. Alveolar cell enlargement
Wilder, 1963 (34)	Dogs, N=9	5×2 cm amputation of upper lobe	No drains left in place, 6/9 animals survived (compared to 3/9 in glue-treated group). In survivors, lesions were adherent to chest wall	ND
Poticha, 1965 (18)	Dogs, N=6	Removal of entire parietal surface of lobe at 3 mm depth	No drains left in place, no air leak complications. One death due to other pulmonary complications. Exudate of blood and fibrin sealed all air leaks, at 1 week leading to fibrin adhesions to chest wall and atelectasis adjacent the injury	ND
Nuchprayoon, 1968 (35)	Dogs, N=8	Removal of lung tissue at costophrenic margin at 1.5–2 cm depth, inducing 12×1.5 cm raw surface	Bronchi >1.0 mm suture ligated and three hours thoracic drainage postoperatively. 6/8 animals died due to tension pneumothorax. 2/8 developed chronic lower lobe atelectasis due to air leak	Alveolar congestion
McCarthy, 1988 (24)	Dogs, N=8	9×9 cm defect at 0.5 cm depth on left lower lobe	Air leak sealed on thoracic drainage in 4/8 control animals (also in 4/8 sealed animals)	ND
Feito, 2000 (37)	Rabbits, N=10	Several superficial incisions (average 7) at 1.5 mm depth	Uneventful postoperative course in all animals. At day 0–1, mean 19.4% pneumothorax, reduced to 3.3% at day 6–7. Adhesions present at obduction	ND
Luh, 2004 (40)	Pigs, N=5	Bilateral 5×5 cm <0.5 cm depth lesions on left and right upper lobes	Critical leak pressure <5 mmHg at 0.5 and 72 h. Air leakage on thoracic drain until 72 h	Poor pleural coverage
Getman, 2006 (38)	Rats, N=10	5 mm parietal defects	Uneventful postoperative course. Adhesions of defect area to chest wall	ND
Kanzaki, 2007 (36)	Rats, N=4	5 mm long incision at 3 mm depth	4/4 animals died due pneumothorax within 1 h	ND
Buyukkale, 2017 (39)	Rats, N=8	Linear incision left upper zone 0.2×0.1 cm (length × height)	No postoperative complications. Air leak pressure mean 43.5 mmHg at day 7	ND

[a], species used not well described in paper; [b], since sutures were used, healing cannot be attributed to intrinsic sealing. However, histology findings were representative of intrinsic sealing mechanisms in this study. ND, not described; BPF, bronchopleural fistula.

https://dx.doi.org/10.21037/jtd-23-180